



OPEN

Functionalized graphene/ polystyrene composite, green synthesis and characterization

Rania Farouq

A composite of sulfonated waste polystyrene (SWPS) and graphene oxide was synthesized by an inverse coprecipitation in-situ compound technology. Polystyrene (PS) has a wide range of applications due to its high mechanical property. The graphene was incorporated into sulfonated polystyrene (SPS) to improve the thermal stability and mechanical performance of the composites. Functionalized graphene was synthesized with a four-step method by using a recovered anode (graphite) of dry batteries while sulfonated waste expanded polystyrene was obtained through sulfonation of the polymer. The SPS and GO + SPS composite were characterized using Fourier Transform Infrared spectroscopy (FT-IR) and transmission electron microscopy (TEM). While the degree of sulfonation (DS) was determined through elemental analysis. The results show the degree of sulfonation of the composite is 23.5% and its ion exchange capacity is 1.2 meq g^{-1} . TEM analysis revealed that the GO particles were loaded on the surface of sulfonated polystyrene and that the SWPS was intercalated into the sub-layers of nanoG homogeneously, which results in an increase in electrical conduction.

With up to millions tonnes of plastic released up to now, plastic garbage is becoming a significant environmental concern. Of these waste streams, one of the largest is that of polystyrene (PS), with an annual production rate exceeding 20 million tons per year¹, waste polystyrene can be chemically modified through various processes like sulfonation^{2,3}. Hydrophilicity, proton conductivity, ion exchange capacity, and water solubility are improved when polymers are sulfonated⁴⁻⁷. Biocompatible electrodes, stimuli-responsive photonic crystals, humidity sensors, parts of photovoltaic systems, ion exchange membranes, flocculant compound for water treatment, and catalysts are just a few of the uses for sulfonated waste polystyrene^{3,8}.

Dry cell batteries are extensively employed in different home applications. These batteries cannot be recharged and must be disposed after they have been totally consumed. Huge amounts of spent battery wastes are produced, which need to be recycled to preserve raw materials in the interest of sustainable development^{9,10}. The most of battery recycling technologies focus only on recovering precious metals such as Zn, Mn, Fe, and other metals. The graphite in the batteries is burned, left as residue, or ignored throughout the manufacturing process. Anyone considering recycling or reusing these batteries should consider the graphite rod located in the battery's core¹¹. Graphene is drawing attention as a catalyst support because of its stability and compatibility with a wide range of catalytically active particles¹². Negatively charged groups on a functionalized graphene surface such as graphene oxide (GO), interfere with dyes, metallic ions, and organic compounds¹³. The high conductivity of graphene oxide can aid electron transport during transformations¹⁴.

The interaction between graphene and the supported metal catalyst is usually weak due to the chemically inert nature of graphene, and thus defects and functional groups are instilled to improve this interaction¹⁵.

GO improves the thermal, electrically conductive, electrochemical and adsorptive properties of polymer composites (Hierarchical assembly of polystyrene/graphitic carbon nitride/reduced graphene oxide nanocomposites toward high fire safety). Graphene oxide (GO) nanosheets used in a membrane matrix demonstrated positive effects on the performance of fuel cells¹⁶. Its large surface area with many polarized groups may help to construct continuous proton transport channels and resist the transportation of methanol, so a small amount of GO could be beneficial for improving the proton conducting behaviors and lower the methanol permeability¹⁷.

The most widely used Hummers' method for synthesis of GO involved the treatment of graphite with KMnO_4 and NaNO_3 , which is considered to be hazardous. When compared to Hummers' technique, Tour employs H_3PO_4 , a weak acid with minimal toxicity and no risk of gas release. It is also regarded to be more sustainable¹⁸. This technique produces a graphite oxide that is more oxidized with a more regular carbon skeleton¹⁹⁻²¹. In this work, we first utilized an environmentally friendly route to prepare a graphene derivative (graphene oxide, GO). The GO

Petrochemical Engineering Department, Pharos University in Alexandria, Alexandria, Egypt. email: rania.farouq1981@gmail.com

was then incorporated into the SWPS particles which can be used as ion exchange. Although ion exchange is one of the most efficient methods for heavy metal removal, with technologically simple operation, high efficiency and reliability. However, due to the high cost of ion exchange resins, the ion exchange process is not commonly used for industrial wastewater treatment. So using recycled materials as ion exchange resins are also a possible solution for cost reduction production and application of ion exchange resins. The composite of sulfonated waste polystyrene and graphene oxide nanoparticles was synthesized and characterized.

Materials and methods

Extraction of graphite from waste dry cell batteries. The spent batteries were carefully disassembled without causing any damage to the graphite rods within. To remove the other chemicals adhered to the graphite rods, they were disassembled and thoroughly wiped and washed with distilled water. After drying, the electrodes were ground and crushed to produce a fine graphite powder. Further treatment of the graphite powder was carried out in a beaker, containing HCl and HNO₃ (3:1) and heated for 6 h. Finally, to get the pH back to normal, the sample was centrifuged and rinsed multiple times in distilled water. Recovered graphite powder [G (R)] was dried at 60 °C for 24 h.

Preparation of graphene oxide by a modified hummer's method. Graphene oxide (GO) was synthesized from graphite powder using a modified hummers technique in a conventional approach. Sulfuric acid (H₂SO₄) and phosphoric acid (H₃PO₄) (ratio 9:1) were blended for few minutes. Then, 3.75 g of graphite was added to the reaction mixture while stirring. After that, 22.5 g of potassium permanganate (KMnO₄) was gently added to the mixture. The solution was agitated for 24 h until it turned dark green. 30 ml hydrogen peroxide (H₂O₂) was dropped gently and agitated for 10 min to remove excess KMnO₄. The reaction is exothermic so it was allowed to cool down. 400 ml of equal volumes of hydrochloric acid (HCl) and deionized water mixture was added and centrifuged for 20 min at 5000 rpm. The solution was then decanted away, and the residuals were rewashed three times with HCl and water. Then the solution was dried at 90 °C for 24 h.

Preparation of sulfonated polystyrene (SPS). Waste EPS packaging material was collected washed, and air dried. It was ground in a seed mill until the pieces were from 3 to 7 mm wide with a thickness of 1 mm. The resulting polystyrene was sulfonated in two stages by reaction with acetyl sulfate in CH₂Cl₂, according to the following sulfonation process:

Preparation of acetyl sulphate (sulfonation reagent). This step should be done freshly prior to the sulfonation reaction of PS. 12 mL of acetic acid anhydride were mixed with 24 mL of dichloroethane, in three-neck flask under nitrogen atmosphere. This solution is cooled to 0 °C in ice bath. Then, 6 mL of Oleum were added portion-wise and stirred for 1 h while maintaining the temperature, resulting in 1 M of acetyl sulphate (homogeneous and clear solution).

Note: during the preparation an excess of acetic anhydride were used to make sure that there are no water traces, and that the latter was completely converted to [acetyl sulphate]. Finally, the three-neck flask was capped, and the acetyl sulphate resulted in DCE solution was ready to be used.

Sulfonation reaction. 4 g of PS were completely dissolved with 200 mL of dichloroethane in a 500 mL three-neck flask, equipped with a condenser, mechanical stirring, thermometer and dropping funnel. The solution was stirred at 40 °C under a small nitrogen flow rate, until a homogeneous solution is attained. As prepared 1 M acetyl sulphate was immediately transferred and added to the polymer solution at (40 °C) using a dropping funnel. The degree of sulfonation of PS was controlled by adjusting the sulfonation time from 1 to 6 h, the solution became clear yellow colour after the addition of sulfonating agent. The reaction was stopped by adding 10 mL of isopropanol to the mixture and allowing it to cool to room temperature. Next step was precipitation by dropping the prepared solution into a large volume of boiling deionized water. Followed by washing several times with deionized water to eliminate the solvent and hydrolyse the acetyl sulphate. Finally, the obtained powder was filtered and dried at (70 °C) in a vacuum oven for 3 days.

Synthesis of GO + SWPS composites. Inverse coprecipitation in-situ compound method was used to form SPS/GO composites as shown in Fig. 1. 2 g SPS particles and 40 mL of 0.2 M NaOH solution were transferred to a 250 mL four-neck flask and kept at 80 °C for 30 min. Throughout the reaction, N₂ was bubbled. Then, using an ultrasonic disperse technique, 0.0164 g GO were dispersed into 60 mL 1:1 (V/V) ethanol–water mixed solvents. After that, the mixture was dropped into the above four-neck flask and vigorously stirred for 30 min at 80 °C. The suspension's colour changed to black almost instantly. When the dropping was done, the stirring was maintained at 50 °C for 1 h. The composite was isolated by centrifuge after cooling to room temperature, rinsed with deionized water until the solution was neutral, then dried under vacuum at 60 °C for 24 h²¹.

Results & discussion

Reaction scheme of homogeneous sulfonation. The sulphonation process occurs in two steps: Fig. 2 depicts the reaction involved in homogeneous sulfonation of PS, and Fig. 3 depicts the homogeneous sulfonation reaction scheme.

Sulfonation reaction might take longer than expected because of a side reaction for sulfonate synthesis induced by a crosslinking event that occurred between two sulfonic groups for distinct SPS units due to an intermolecular mechanism. Figure 4 depicts the crosslinking mechanism.

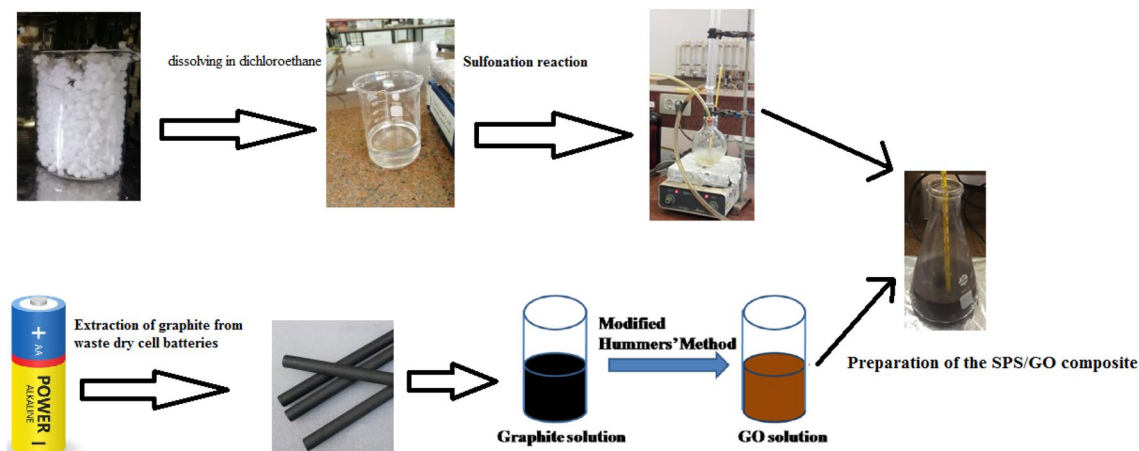


Figure 1. Synthesis of GO + SWPS composites.

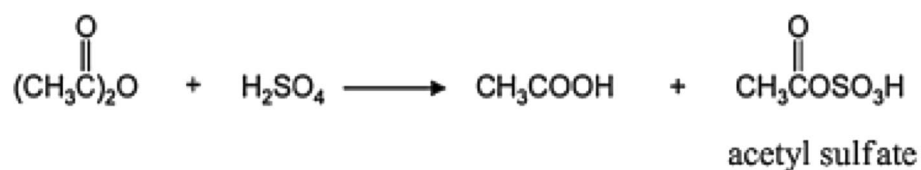


Figure 2. the reactions involved in the homogeneous sulfonation of PS.

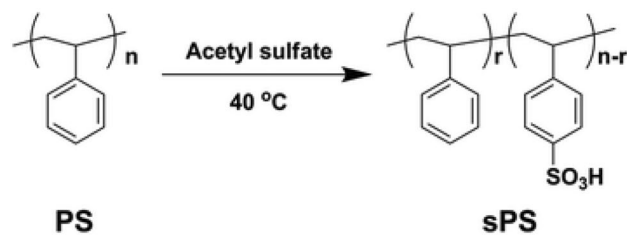


Figure 3. Reaction scheme of homogeneous sulfonation.

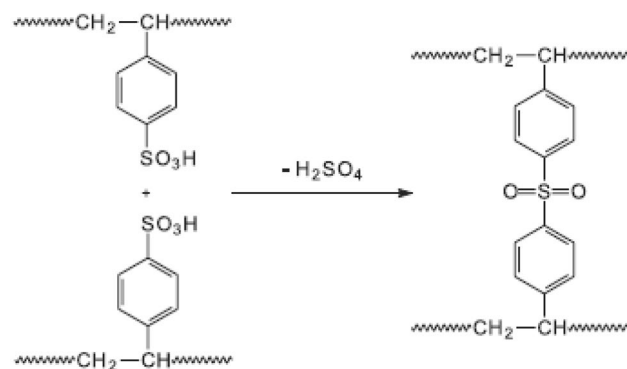


Figure 4. Crosslinking reaction of two sps groups.

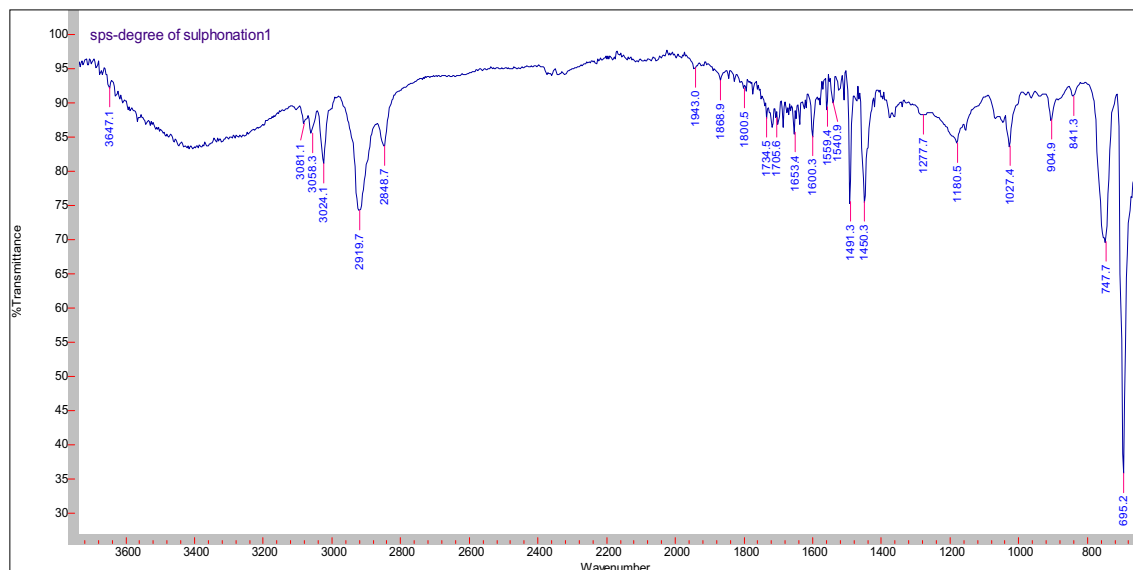


Figure 5. FTIR spectra of the sulfonated polystyrene.

Tendency to the inter-molecular reaction is affected with several parameters including:

1. The sulfonic groups content will be increased by the elevating the concentration for the reaction sulfonating agent used with polymer solution.
2. Also elevating reaction temperature will lead to a higher percentage of the yields

The best degree of sulfonation 30% was found to be achieved after 3 h²².

FT-IR characterization. There are principle peaks found in sulfonated polystyrene represented in Fig. 5, the band characteristic of the aromatic =C–H stretching band at 3024.1 cm⁻¹, the band characteristic of the symmetrical stretch of CH₂ is also observed in 2848.7 cm⁻¹ –CH₂–asymmetric stretching sharp peak a 2919.7 cm⁻¹, C=C para–disubstituted benzene at 1450.3 cm⁻¹, The vibration of the aromatic skeleton is found in the band at 1600 cm⁻¹, The bands between 904.9 and 695.2 cm⁻¹ are associated with vibration of C–H deformation of the aromatic ring which are characteristic to polystyrene.

The peak at 3647.1 cm⁻¹ belongs to O–H in the sulfonic acid groups, stretching vibration of S=O at 1180.5 cm⁻¹, and symmetric stretching of the O=S=O at (1027.4) indicates qualitatively the presence of the attached –SO₃H groups in each of sulfonated samples. The band related to the substituted benzene in the para position (841.3 cm⁻¹) validates the aromatic ring substitution.

Because both SPS and GO contain a large number of functional groups on their surfaces, it's possible to predict significant interactions between the two to cause composite production. Actually, as evidenced by the IR data described below, this is proven to be accurate. Figure 6 depicts the key stretching frequencies of SPS/GO. Both SPS and GO peaks are observed in the composite, suggesting that both components are present. The O–H stretching of –SO₃H of SPS at 3647.1 cm⁻¹ shifted to lower wavenumber (3511.6 cm⁻¹) and becomes broader in case of composite attributing that –SO₃H of SPS is involved in the hydrogen bonding interactions with GO particles. Similarly the shifting of asymmetric stretching of –SO₃H of SPS from 1180.5 to 1094.7 cm⁻¹ in composite indicates the presence of hydrogen bonding interactions between the SPS and GO. Also, a substantial shift (695.2–660.7 cm⁻¹) of out of plane bending vibration of PS ring in case of composite is the indication of π – π interactions between the PS backbone and basal planes of graphene. These findings clearly show significant interactions between SPS and GO, which resulted in the formation of a stable composite. The peak of GO is due to C–OH stretching is observed at wavenumber at 1253 cm⁻¹

Structural studies of SPS/GO composites: TEM analysis. TEM were used to analyze the structure of the as-prepared composite. The sample was dissolved in little amount of DMF and the solution is diluted with water and then the TEM samples were prepared by drop casting samples on the carbon coated copper (200 mesh) grid.

These results are in accordance with the TEM image of SPS/GO composite observation. In Fig. 7a, it can be seen that particles were loaded on the surface of sulphonated polystyrene exhibiting a homogeneous distribution with no aggregation compared to Fig. 7b of the GO which shows the linear deposit, exhibiting clear coagulation. The GO-SPS show the few-layered graphene oxide grafted with branches of SPS. This indicates that SPS particles are effectively coated by GO particles.

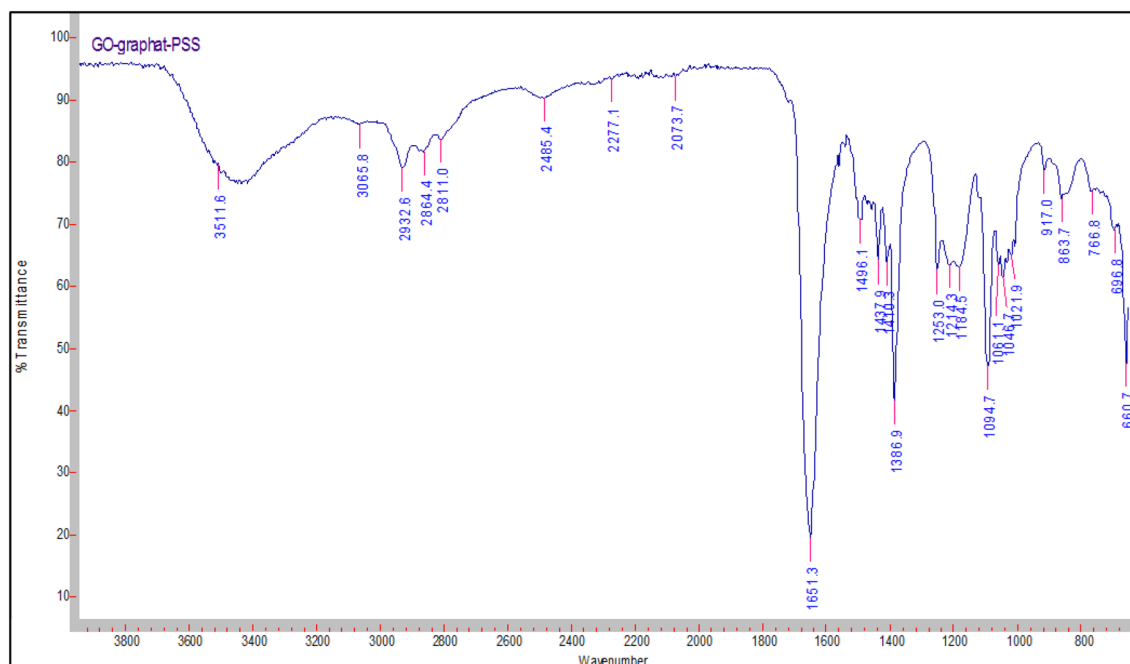


Figure 6. FTIR spectra of the SPS/GO composite.

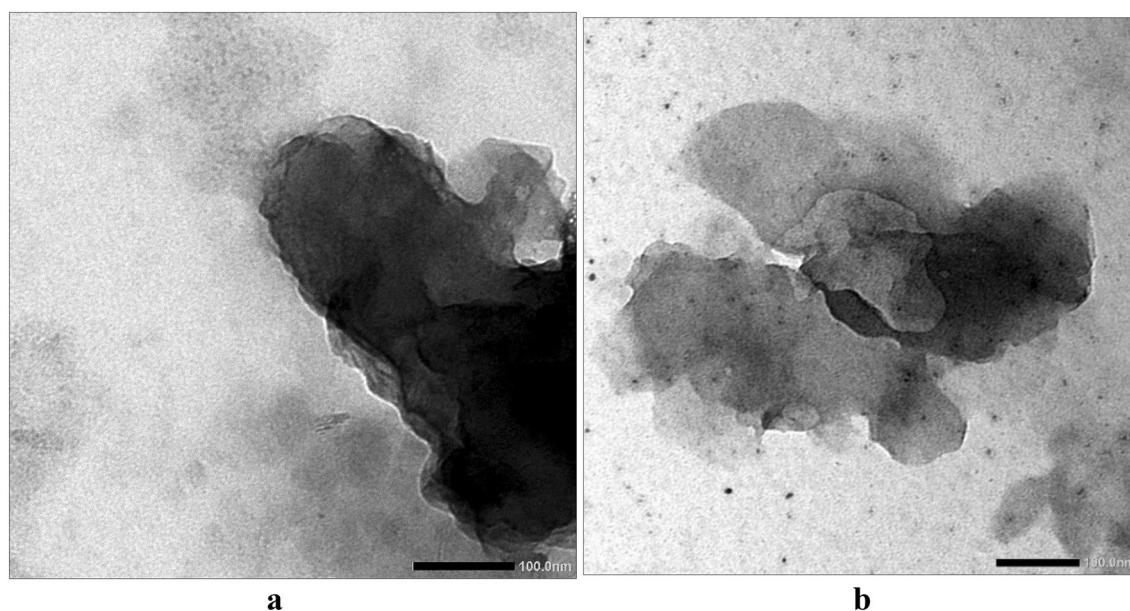


Figure 7. TEM analysis depicting the distribution of (a) graphene oxide (GO) (b) GO/SPS.

The degree of sulfonation (DoS). The resulting SPS was determined by titration. A predetermined amount of SPS were dispersed into 50 mL of distilled water with ultrasonication and vigorous agitation for 30 min. Two droplets of phenolphthalein solution were added. The mixture was titrated by NaOH solution. The consumed volume of NaOH solution was recorded. The DoS was calculated by following Eq.:

$$DoS = V_{NaOH} * C_{NaOH} / M \quad (1)$$

where C_{NaOH} is the concentration of NaOH and M is the mass of SPS.

As the number of sulfonic acid groups linked to the PS has increased, the SPS is more soluble in water and better able to interact with the graphene. As a result of the high degree of substitution of PS by sulfonic acid groups, the phenyl groups can exhibit a conjugation effect with sulfonic acid groups, confirmed by the increased electrical conductivity of the SWPS matrix. As the sulfonation increases, and the sulfonic groups interconnect result in the creation of ionic nanochannels. Those ionic nanochannels are critical for the transport and mechanical properties of the polymer²³.

DS depends largely on many factors such as the concentration of polymer, concentration of the sulfonating agent, the temperature and the time of sulfonation reaction. Indeed, the degree of sulfonation could be controlled by adjusting these parameters. It was clear that, as the sulfonation reaction time was increased, a noticeable increase in DS²⁴.

Conclusions

A composite of graphene oxide (GO) and sulfonated polystyrene are prepared with enhanced properties. The manufacture of SPS was observed in the Fourier transform infrared spectra FT-IR as created function group peak vibration range. The properties of SPS are favourably manipulated by the incorporation of GO. Intermolecular interactions between the components in composite are established by FTIR. Composite is characterized by transmission electron microscopy (TEM) which showed the uniform distribution of GO particles in SPS matrix.

Because of the strong interaction between $-\text{SO}_3\text{H}$ functionality of SPS and functional group of GO, the SPS particles are adsorbed on the graphene surface. This results in stable SPS/GO composite. The composite display better thermal, mechanical and electrical conduction compared to polymer.

SPS particles help to produce and stabilize single layer graphene sheets; in turn these GO Sheets help to produce mechanically strong ion conducting SPS resin. This enhancement allows us to use it for waste water treatment as durable and efficient raw material able to stand in severe conditions. The method we proposed in this paper is a high standard method with several advantages, including the use of waste polystyrene, which reduces environmental pollution, avoids harmful gases, which are environmentally beneficial, and is a convenient and straightforward procedure that saves energy resources. We hope for more practical time leading us for more detail and results but COVID-19 waste mostly available time to finish this study.

Data availability

The datasets used and/or analyzed during the current study available from the corresponding author on reasonable request.

Received: 19 July 2022; Accepted: 13 December 2022

Published online: 16 December 2022

References

- Yang, S. S. *et al.* Biodegradation of polystyrene wastes in yellow mealworms (larvae of *Tenebrio molitor* Linnaeus): Factors affecting biodegradation rates and the ability of polystyrene-fed larvae to complete their life cycle. *Chemosphere* **191**, 979–989 (2018).
- Tran, A. T. *et al.* From waste disposal to valuable material: Sulfonating polystyrene waste for heavy metal removal. *J. Environ. Chem. Eng.* **8**(5), 104302 (2020).
- Andrade, B. T. N. C., Bezerra, A. C. D. S. & Calado, C. R. Adding value to polystyrene waste by chemically transforming it into sulfonated polystyrene. *Matéria (Rio de Janeiro)* <https://doi.org/10.1590/s1517-707620190003.0732> (2019).
- Ding, L., Song, X., Wang, L. & Zhao, Z. Enhancing proton conductivity of polybenzimidazole membranes by introducing sulfonate for vanadium redox flow batteries applications. *J. Membr. Sci.* **578**, 126–135 (2019).
- Purbowatinigrum, R. S., Prasetya, N. B. A., Kusworo, T. D. & Susanto, H. Sulfonated polystyrene and its characterization as a material of electrolyte polymer. *J. Phys. Conf. Ser.* **1025**(1), 012133 (2018).
- Jalal, N. M., Jabur, A. R., Hamza, M. S. & Allami, S. Sulfonated electrospun polystyrene as cation exchange membranes for fuel cells. *Energy Rep.* **6**, 287–298 (2020).
- Dai, Z., Ansaloni, L., Ryan, J. J., Spontak, R. J. & Deng, L. Incorporation of an ionic liquid into a midblock-sulfonated multiblock polymer for CO₂ capture. *J. Membr. Sci.* **588**, 117193 (2019).
- Hussain, S. *et al.* Photothermal responsive ultrathin Cu-TCPP nanosheets/sulfonated polystyrene nanocomposite photo-switch polymer conducting membranes. *J. Membr. Sci.* **620**, 118888 (2021).
- Ali, G. A., Yusoff, M. M., Shaaban, E. R. & Chong, K. F. High performance MnO₂ nanoflower supercapacitor electrode by electrochemical recycling of spent batteries. *Ceram. Int.* **43**(11), 8440–8448 (2017).
- Sadeghi, S. M., Jesus, J. & Soares, H. M. A critical updated review of the hydrometallurgical routes for recycling zinc and manganese from spent zinc-based batteries. *Waste Manag.* **113**, 342–350 (2020).
- Bandi, S., Ravuri, S., Peshwe, D. R. & Srivastava, A. K. Graphene from discharged dry cell battery electrodes. *J. Hazard. Mater.* **366**, 358–369 (2019).
- Zhang, K. *et al.* Copper oxide-graphene oxide nanocomposite: Efficient catalyst for hydrogenation of nitroaromatics in water. *Nano Converg.* **6**(1), 1–7 (2019).
- Tu, T. H., Cam, P. T. N., Phong, M. T., Nam, H. M. & Hieu, N. H. Synthesis and application of graphene oxide aerogel as an adsorbent for removal of dyes from water. *Mater. Lett.* **238**, 134–137 (2019).
- Zhou, D. *et al.* NiCoFe-layered double hydroxides/N-doped graphene oxide array colloid composite as an efficient bifunctional catalyst for oxygen electrocatalytic reactions. *Adv. Energy Mater.* **8**(9), 1701905 (2018).
- Ahmad, H., Fan, M. & Hui, D. Graphene oxide incorporated functional materials: A review. *Compos. B Eng.* **145**, 270–280 (2018).
- Zakaria, Z. & Kamarudin, S. K. Evaluation of quaternized polyvinyl alcohol/graphene oxide-based membrane towards improving the performance of air-breathing passive direct methanol fuel cell s. *Int. J. Energy Res.* **44**(11), 8988–9000 (2020).
- Yang, T. *et al.* A graphene oxide polymer brush based cross-linked nanocomposite proton exchange membrane for direct methanol fuel cells. *RSC Adv.* **8**(28), 15740–15753 (2018).
- Yadav, N., Kallur, V., Chakraborty, D., Johari, P. & Lochab, B. Control of functionalities in GO: Effect of bronsted acids as supported by ab initio simulations and experiments. *ACS Omega* **4**(5), 9407–9418 (2019).
- Sali, S., Mackey, H. R. & Abdala, A. A. Effect of graphene oxide synthesis method on properties and performance of polysulfone-graphene oxide mixed matrix membranes. *Nanomaterials* **9**(5), 769 (2019).
- Chang, W. T. *et al.* Graphene oxide synthesis using microwave-assisted versus modified Hummer's methods: Efficient fillers for improved ionic conductivity and suppressed methanol permeability in alkaline methanol fuel cell electrolytes. *J. Power Sour.* **414**, 86–95 (2019).
- Ma, Y. *et al.* One-pot method fabrication of superparamagnetic sulfonated polystyrene/Fe₃O₄/graphene oxide micro-nano composites. *J. Porous Mater.* **25**(5), 1447–1453 (2018).
- Martins, C. R., Ruggeri, G. & De Paoli, M. A. Synthesis in pilot plant scale and physical properties of sulfonated polystyrene. *J. Braz. Chem. Soc.* **14**, 797–802 (2003).

23. Suleiman, D. *et al.* Mechanical and chemical properties of poly (styrene-isobutylene-styrene) block copolymers: Effect of sulfonation and counter ion substitution. *J. Appl. Polym. Sci.* **131**(11), n/a (2014).
24. Jalal, N. M., Jabur, A. R., Hamza, M. S. & Allami, S. (2020). The effect of sulfonation reaction time on polystyrene electrospun membranes as polymer electrolyte. In *AIP Conference Proceedings* (Vol. 2290, No. 1, p. 020049). AIP Publishing LLC.

Author contributions

R.F. has wrote the main manuscript text, prepared figures and reviewed the manuscript.

Funding

Open access funding provided by The Science, Technology & Innovation Funding Authority (STDF) in cooperation with The Egyptian Knowledge Bank (EKB).

Competing interests

The author declares no competing interests.

Additional information

Correspondence and requests for materials should be addressed to R.F.

Reprints and permissions information is available at www.nature.com/reprints.

Publisher's note Springer Nature remains neutral with regard to jurisdictional claims in published maps and institutional affiliations.



Open Access This article is licensed under a Creative Commons Attribution 4.0 International License, which permits use, sharing, adaptation, distribution and reproduction in any medium or format, as long as you give appropriate credit to the original author(s) and the source, provide a link to the Creative Commons licence, and indicate if changes were made. The images or other third party material in this article are included in the article's Creative Commons licence, unless indicated otherwise in a credit line to the material. If material is not included in the article's Creative Commons licence and your intended use is not permitted by statutory regulation or exceeds the permitted use, you will need to obtain permission directly from the copyright holder. To view a copy of this licence, visit <http://creativecommons.org/licenses/by/4.0/>.

© The Author(s) 2022